



Research article

Removal of Methylene Blue from a synthetic effluent by ionic flocculation

Yago Neco Teixeira^{a,b}, Francisco José de Paula Filho^{a,b,*}, Vinícius Pereira Bacurau^c,
Jorge Marcell Coelho Menezes^b, Anderson Zhong Fan^c, Ricardo Paulo Fonseca Melo^d

^a Agrarian Sciences and Biodiversity Center, Federal University of Cariri, Ícaro Moreira de Sousa St, 126, 63130-025, Crato, Ceará, Brazil

^b Science and Technology Center, Federal University of Cariri, Av. Ten. Raimundo Rocha, 1639, 63048-080, Juazeiro do Norte, Ceará, Brazil

^c Materials Engineering Department, Federal University of São Carlos, Rod. Washington Luiz, 235, 13565-905, São Carlos, São Paulo, Brazil

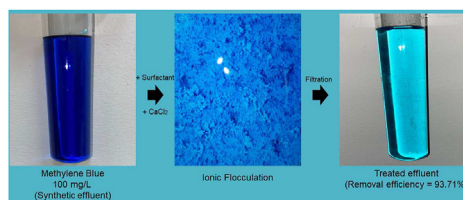
^d Exact and Natural Sciences Department, Federal University of Semi-Árido, BR 226, n-n, 59900-000, Pau dos Ferros, Rio Grande do Norte, Brazil



HIGHLIGHTS

- Ionic flocculation is a simple, inexpensive and highly efficient process.
- Biodegradable and sustainable surfactant.
- Fast and high removal of Methylene Blue (0.5 min–93.71%).
- Process of exothermic nature.

GRAPHICAL ABSTRACT



ARTICLE INFO

Keywords:
Methylene Blue
Surfactant
Ionic flocculation
Adsorption
Desorption

ABSTRACT

Methylene Blue (MB) is a dye widely used in the industrial sector and in human and veterinary pharmacology. This dye, if improperly disposed of, can cause a significant environmental impact due to its low biodegradability, as it is a stable and complex substance. Additionally, it may affect human health and generate highly toxic byproducts. Hence, the purpose of this work is to assess the removal efficiency of MB from a synthetic effluent using an ionic flocculation process. Such a process consists of the dissolution of a biodegradable anionic surfactant (obtained from soybean oil used for frying food) in the synthetic effluent and the subsequent addition of calcium to the system. The addition of Ca leads to the formation of insoluble surfactant flocs with a high capacity to adsorb organic pollutants. The FTIR testing showed the presence of OH^- and C=O groups in the surfactant flocs, which favor the removal of MB by an adsorption process. The maximum adsorption capacity of MB was 101.38 mg g^{-1} . The process is in fact a chemisorption and has an exothermic nature. Desorption studies showed a desorption efficiency of up to 47.81% using an ethanol 1:2 solution. An MB removal efficiency of up to 93.71% was attained in just 0.5 min for an initial MB concentration of 100 mg L^{-1} , showing that ionic flocculation is a very fast and effective process for the treatment of effluents.

1. Introduction

The treatment of dye-containing effluents is a daily concern in industrial facilities because of the aesthetic impact and potential toxicity problems. Dyes affect the environment mainly because they are difficult to degrade, as they are relatively stable compounds [1].

MB is a cationic dye used as a coloring agent for paper and fabrics [2]. Moreover, MB has also been used in human and veterinary pharmacological products for a long time [3, 4]. MB is known to cause disorders in humans and to generate highly toxic byproducts such as sulfur and nitrogen oxides, facts that have rendered its removal from effluents mandatory [5, 6, 7, 8, 9].

* Corresponding author.

E-mail address: francisco.filho@ufca.edu.br (F.J. de Paula Filho).

<https://doi.org/10.1016/j.heliyon.2022.e10868>

Received 29 June 2022; Received in revised form 8 September 2022; Accepted 27 September 2022

2405-8440/© 2022 Published by Elsevier Ltd. This is an open access article under the CC BY-NC-ND license (<http://creativecommons.org/licenses/by-nc-nd/4.0/>).

Dyes cannot be completely removed from effluents through conventional processes (activated sludge and anaerobic digestion) due to their low biodegradability and complex structure [10]. Therefore, finding more adequate methods, more efficient and less costly, is essential.

Among several techniques currently used for the removal of dyes from effluents, the following can be highlighted: Fenton reaction [11], gels and hydrogels [12, 13], biocomposites films [14], photo-catalytic degradation [15], modified membranes [16, 17], ultrafiltration [18, 19], flocculation [20, 21], and adsorption.

Adsorption is an efficient treatment method widely explored due to its low cost, simple operation and high efficiency. With that in view, different materials have been used to remove MB from effluents by adsorption, such as fresh bamboo [22], activated carbon [2], kaolin [10], fly ash [9], anodic sludge [23], and modified manganese [24].

The use of surfactants (SF) for the removal of MB is a viable alternative as they can be obtained from low-cost raw materials. SFs are amphiphilic substances in which the polar part is responsible for the molecule's affinity for water and the nonpolar part interacts with nonpolar substances.

The addition of calcium (Ca^{2+}) to the SF + effluent solution leads to the formation of insoluble SF salts, a process known as ionic flocculation. These salts appear in the form of surfactant flocs which, in turn, have a significant decontamination potential for organic compounds [25].

The SF produced from vegetable oils does not have branched carbon chains or aromatic groups attached and, consequently, is biodegradable [26, 27]. In addition, the positive profile of this product's ecological and sustainable impact cannot be stressed enough, as it does not generate byproducts that are harmful to the environment.

Another advantage of this SF is that it is obtained from used frying soybean oil, giving thus an adequate destination to a domestic/industrial waste that has a low biodegradability and is capable of harming aqueous ecosystems and living organisms like terrestrial plants and animals.

Therefore, this work aims to study the efficiency of MB removal by ionic flocculation, promoted by the use of SF originated from frying soybean oil. Also intend to analyze the influence of pH, temperature and electrolytes on the process, establish the adsorption parameters, and analyze the desorption process. It is worth mentioning that this is the first time that frying soybean oil is used as a raw material to promote ionic flocculation, presenting advantages such as: low cost (since it is a waste commonly improperly disposed of in the environment), high removal efficiency at low and high concentrations of MB, simple and fast process, and its biodegradability.

2. Methodology

2.1. Surfactant production

The SF used in this study was synthesized in the laboratory from frying soybean oil and potassium hydroxide (KOH), using a mass ratio of 79.35% and 20.65%, respectively. This ratio was based on the saponification index of the oil. Initially, the masses of oil and KOH (146 g and 38 g, respectively) were weighted. Then, the oil was diluted in 24 mL of ethyl alcohol and the KOH in 33 mL of distilled water. Soon after that, the solutions were mixed in a 500 mL beaker on a heated magnetic stirrer (100 rpm and 80 °C).

The system was maintained as indicated above until the surfactant was formed, a process that took approximately 40 min (i.e. the period of time upon which the saponification reaction and SF formation was completed). Then, the SF was dried in an oven at 105 °C for 8 h. After drying, the SF was macerated and stored in a suitable plastic container until it was used in the experiment. The open molecular structure of SF is shown in Figure 1.

2.2. Surfactant characterization

Energy dispersive spectroscopy (EDS) (FEI, Inspect S50) tests were conducted before and after the MB adsorption process in order to better understand the composition of the SF flocs.

The SF flocs were also analyzed by Fourier transform infrared (FTIR) spectroscopy (PerkinElmer, Spectrum Two), both before and after the MB adsorption process, in order to identify the surface functional groups. The samples were prepared using KBr pellets and the studied spectrum range was 4000–450 cm^{-1} .

In both cases, the SF flocs were previously dried at room temperature and stored in a desiccator until the testing was performed. The constant solubility product (K_{sp}) of the surfactant is $3.7 \times 10^{-10} \text{ M}^3$ [28].

2.3. Tested parameters

The MB ($\text{C}_{16}\text{H}_{18}\text{N}_3\text{SCl}$, 319.85 g mol^{-1}) adsorption studies were conducted under different experimental conditions. Table 1 summarizes the tested parameters and conditions.

A stock solution of MB with a concentration of 500 mg L^{-1} was prepared by dissolving MB in deionized water. All other MB solutions were prepared by diluting the stock solution.

Except when tested for the effect of pH and electrolytes, the SF was completely dissolved in the MB solutions, followed by the addition of Ca^{2+} . To analyze the pH effect, the pH of the solutions was adjusted with HCl and NaOH solutions (1 mol L^{-1}) immediately after the dissolution of SF and before the addition of Ca^{2+} .

The effect of electrolytes was tested using NaCl, which was dissolved in the solutions after the complete dissolution of the SF and before the addition of Ca^{2+} . This is a crucial parameter in this type of study as industrial effluents generally have high concentrations of electrolytes [29].

Ca^{2+} was added to the solutions as a CaCl_2 solution (0.023 mol L^{-1}). 4 mL of the CaCl_2 solution were used per sample, resulting in a Ca^{2+} concentration per solution of approximately 0.002 mol L^{-1} . This concentration was sufficient to promote the ionic flocculation process.

After each of the steps described above, the SF flocs were separated from the samples using a commercial filter paper. The concentration of MB in the filtered samples was measured using a UV–VIS spectrophotometer (Shimadzu, UV 1800) at a wavelength of 665 nm. All steps were performed in triplicate.

2.4. Contact time and desorption kinetics

The SF dosage was set at 4 g L^{-1} while initial MB concentrations of 10, 50 and 100 mg L^{-1} were studied to determine the equilibrium time. All the other data are outlined in Table 1. The desorption efficiency was analyzed using the same data used for the equilibrium time analysis, with the exception of the initial MB concentration (0 mg L^{-1}) and the pH values of the solution (which varied depending on the eluent used). The following eluents were used for the desorption study: deionized water (pH = 5.54), HCl 0.1 mol L^{-1} , HCl 0.01 mol L^{-1} , NaOH 0.1 mol L^{-1} , ethanol 1:5, and ethanol 1:2.

After the ionic flocculation took place, the MB-adsorbed SF flocs were washed with deionized water, dried at room temperature and stored in a desiccator until the desorption kinetics tests were conducted. Eq. (1) shows how the desorption efficiency (%DES) was calculated:



Figure 1. Molecular structure of SF.

Table 1. Different tested parameters.

Test	SF (g L ⁻¹)	MB (mg L ⁻¹)	Electrolytes (NaCl mol L ⁻¹)	Time (min)	pH	Temp. (°C)	Volume (mL)	Stirring (rpm)
SF dosage, Temperature and Thermodynamics	1-2-3-4	100	0	90	11	10-20-30-40-50-60-70	20	80
pH	4	100	0	90	7-8-9-10-11-12-13	30	20	80
Electrolytes	1-2-3-4	100	0-0.3-0.5	90	11	30	20	80
Contact time	4	10-50-100	0	0.5-1-5-10-20-30-60-90-120-150-180-240-300	11	30	20	80
Isotherms	4	10-50-100-150-200-250-300-350-400	0	90	11	30	20	80

$$\%DES = \left(\frac{C_t}{D_{SF}q_0} \right) 100 \quad 1$$

where: C_t is the MB concentration in the solution at a given time (mg L⁻¹); D_{SF} is the SF dosage (g L⁻¹); and q_0 is the quantity of MB present on the flocs at the initial moment (mg g⁻¹).

2.5. Adsorption isotherms

The adsorption isotherms were studied using the Langmuir (Eq. (2)), Freundlich (Eq. (3)), Temkin (Eq. (4)) and Dubinin–Radushkevich (D–R) (Eq. (5)) non-linear models.

$$q_e = \frac{q_{max}k_L C_e}{1 + k_L C_e} \quad 2$$

$$q_e = k_F C_e^{1/n} \quad 3$$

$$q_e = \frac{RT}{b} \ln(k_T C_e) \quad 4$$

$$q_e = q_m \exp \left\{ -k_{DR} \left[RT \ln \left(1 + \frac{1}{C_e} \right) \right]^2 \right\} \quad 5$$

where: q_e – SF adsorption capacity at the equilibrium time (mg g⁻¹); q_{max} – Maximal adsorption capacity (mg g⁻¹); k_L – Langmuir isotherm constant (L mg⁻¹); C_e – MB concentration at equilibrium in the liquid phase (mg L⁻¹); k_F – Freundlich isotherm constant (mg g⁻¹ (mg L⁻¹)^{-1/n}); n – Constant related to the heterogeneity of the adsorbent's surface; R – Universal gas constant (8.314 J mol⁻¹ K⁻¹); T – Process temperature (K); b – Constant related to the adsorption heat (kJ mol⁻¹); q_m – Maximal theoretical adsorption capacity for the formation of a monolayer (mg g⁻¹); k_{DR} – D–R isotherm constant (mol² kJ⁻²).

The k_L constant is associated to the separation factor or equilibrium parameter (RL), which is a dimensionless constant defined by Eq. (6).

$$RL = \frac{1}{1 + k_L C_0} \quad 6$$

If $RL > 1$, adsorption is not favored; if $RL = 1$, adsorption is linear; if $0 < RL < 1$, adsorption is favored; and if $RL = 0$, adsorption is irreversible [30].

The k_{DR} constant is associated to the mean adsorption energy (E), which can be calculated through Eq. (7).

$$E = \frac{1}{\sqrt{2k_{DR}}} \quad 7$$

where: E is the mean adsorption energy of the process (kJ mol⁻¹). From the value of E , can infer the nature of the process, that is, whether it is a physical adsorption ($E < 8$ kJ mol⁻¹), an ion exchange ($8 < E < 16$ kJ mol⁻¹), or a chemisorption ($E > 16$ kJ mol⁻¹) [31].

2.6. Adsorption thermodynamics

The Gibbs free energy (ΔG°), enthalpy (ΔH°) and entropy (ΔS°) can be calculated from the equilibrium data through Eqs. (8) and (9).

$$\Delta G^\circ = \Delta H^\circ - T\Delta S^\circ \quad 8$$

$$\log \frac{q_e D_{SF}}{C_e} = \frac{\Delta S^\circ}{2.303R} - \frac{\Delta H^\circ}{2.303RT} \quad 9$$

where: q_e – SF adsorption capacity at the equilibrium time (mg g⁻¹); C_e – MB concentration at equilibrium in the liquid phase (mg L⁻¹); R – Universal gas constant (8.314 J mol⁻¹ K⁻¹); T – Process temperature (°K).

ΔH° and ΔS° can be obtained from the angular and linear coefficients, respectively, of the straight line plotted by $\log (q_e D_{SF}/C_e)$ vs $1/T$. Once the values of ΔH° and ΔS° are obtained, ΔG° can be calculated for different temperatures using Eq. (8).

2.7. Removal efficiency

The MB removal efficiency was calculated using Eq. (10):

$$\%Removal = \left(\frac{C_0 - C_e}{C_0} \right) 100 \quad 10$$

where: C_0 – Initial MB concentration in the liquid phase (mg L⁻¹); C_e – MB concentration at equilibrium in the liquid phase (mg L⁻¹).

2.8. Error analysis

The root mean square error (RMSE) (Eq. (11)) was used in order to improve the interpretation of the results and decide which models best fit this study.

$$RMSE = \sqrt{\frac{\sum_1^N [(q_{exp} - q_{cal})/q_{exp}]^2}{N}} \quad 11$$

where: q_{exp} – Experimental adsorption capacity (mg g⁻¹); q_{cal} – Calculated adsorption capacity (mg g⁻¹); N – Number of experimental points.

3. Results and discussion

3.1. Characterization of the SF

The elemental composition of the SF flocs, before and after the adsorption of MB, was determined by EDS (Figures 2a and 2b and Table 2).

Figures 2a, 2b and Table 2 show that SF flocs are basically composed of C (67%), Ca (22.50%) and O (10.10%), with a small percentage of Cu (0.30%) and Si (0.10%). After MB adsorption, the amount of the following elements in the SF flocs increased: C (78.90%), O (14.20%) and

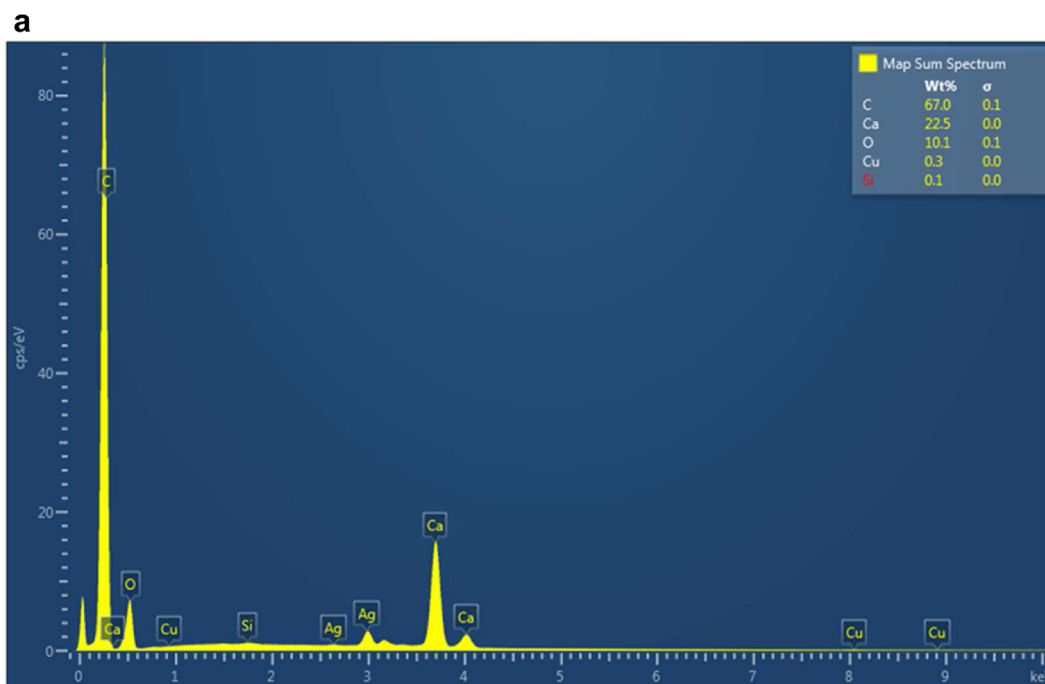


Figure 2a. EDS from surfactant flocs before MB adsorption.

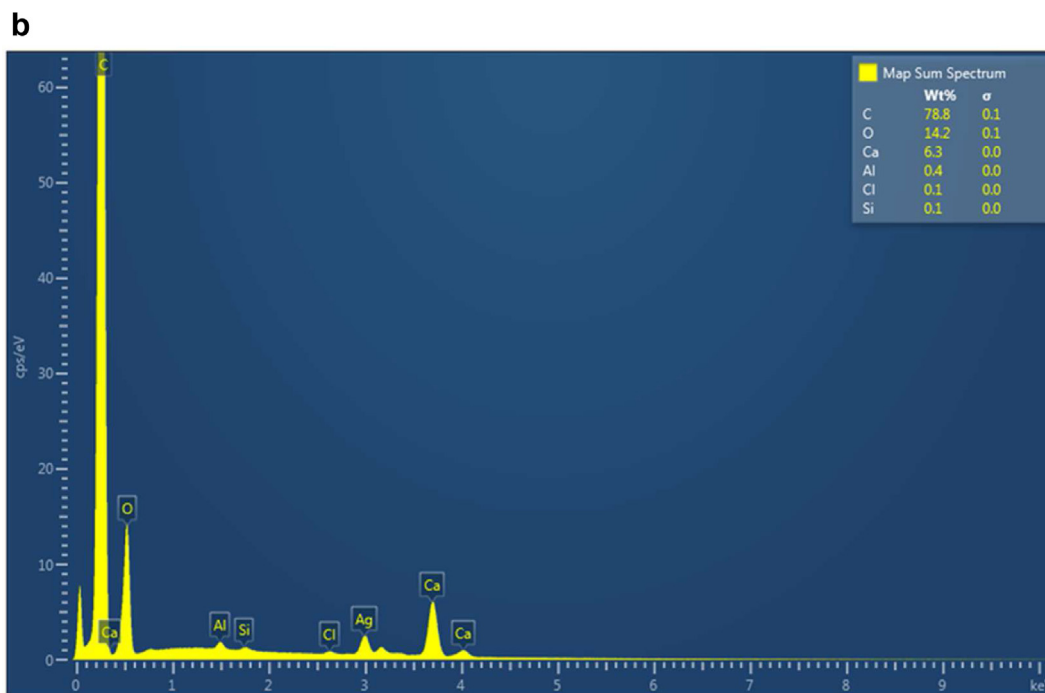


Figure 2b. EDS from surfactant flocs after MB adsorption.

Cl (0.50%). This was due to the interactions between the surface of the SF flocs and MB as, after the adsorption process, part of the dye was removed from the solution and retained on the SF flocs. After the adsorption process, Ca and Cu decreased to 6.30% and 0%, respectively, possibly due to the new bonds formed between SF and MB, promoting a decrease in the percentage of Ca in the SF flocs and its resolubilization in the form of Ca^{2+} [21]. The interaction between SF-MB occurs in the non-polar tails of SF flocs, as these have an affinity for organic compounds. The mechanism of the ionic flocculation process is illustrated in Figure 3.

The FTIR spectra and the main vibration frequencies of the bands for SF, before and after MB adsorption, are shown in Figure 4.

The FTIR analysis confirmed that SF flocs have OH^- and $\text{C}=\text{O}$ functional groups, which favor the adsorption of cationic dyes as these groups are active sites of interaction [32].

Figure 4 shows the presence of hydroxyl groups (OH^-) both before and after the ionic flocculation process, as seen in the region between 3200 and 3600 cm^{-1} , while the OH^- intensity decreased after MB adsorption. This behavior was also observed in the adsorption of MB by activated carbon [32] and alginate beads [33]. A decrease in intensity

Table 2. Elemental composition of the SF flocs.

Elements	SF flocs, before ionic flocculation (%)	SF flocs, after ionic flocculation (%)
C	67.00	78.90
Ca	22.50	6.30
O	10.10	14.20
Cu	0.30	0.00
Si	0.10	0.10
Cl	0.00	0.50
Total	100	100

after the ionic flocculation took place was also noted at the following peaks: 2850-2921.62 cm^{-1} (stretching of C-H, indicating the presence of long-chain linear aliphatic compounds), 1576.48-1578.14 cm^{-1} (R-COOK potassium salts) [34], 1540.39-1541.07 cm^{-1} (stretching of the C=O group), 1419.50-1468 cm^{-1} (CH_2 bending), and 672.38-723.41 cm^{-1} (stretching of -C-Cl). The decrease in intensity at these peaks occurs because of the electrostatic interaction between the MB molecules and the SF flocs, which possibly formed new bonds with these functional groups, making the vibration of these molecules difficult.

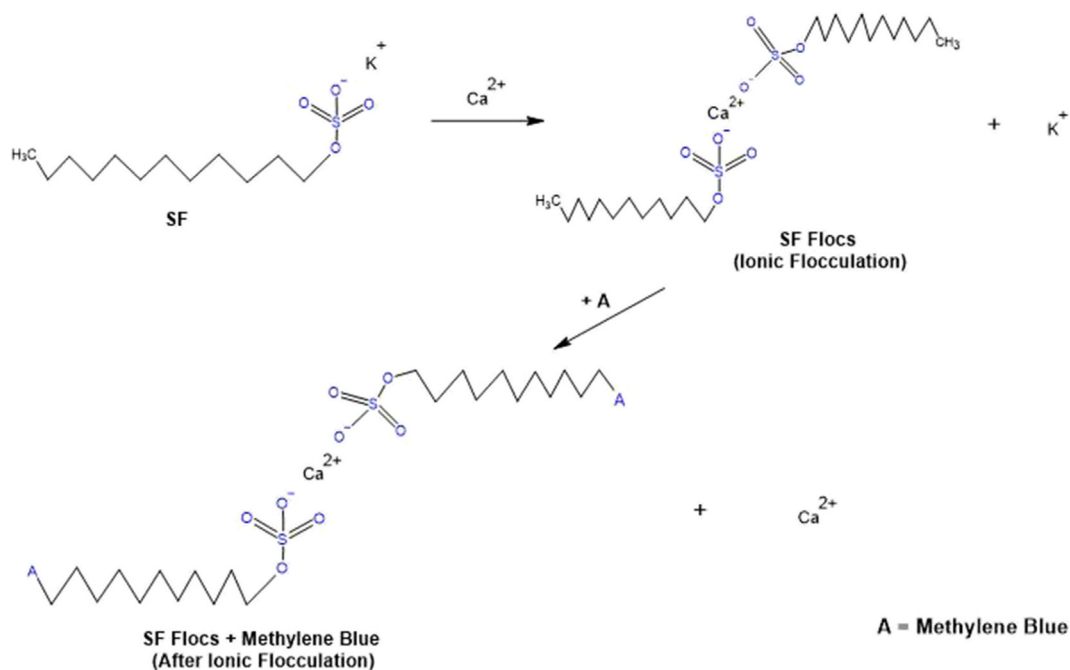


Figure 3. Mechanism of ionic flocculation process.

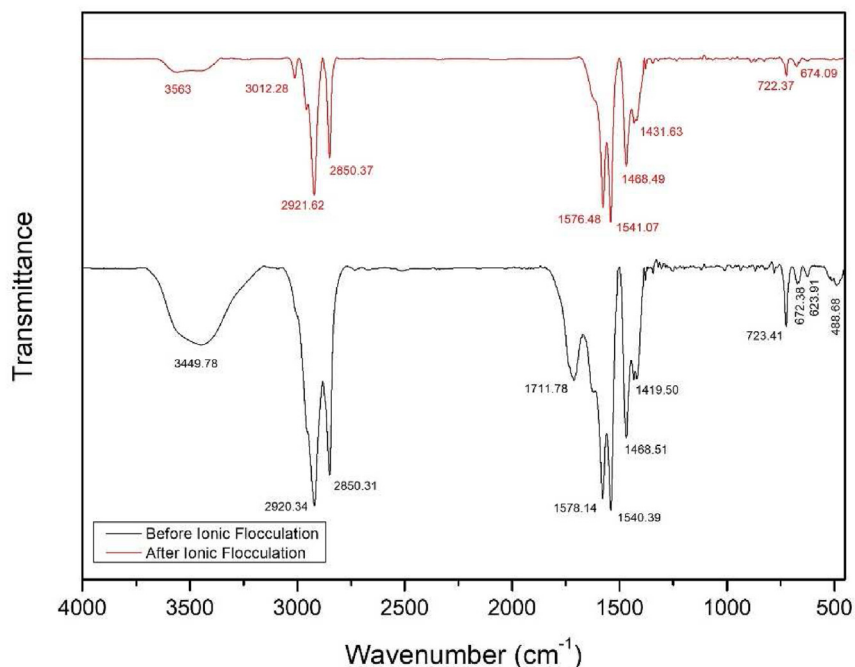


Figure 4. Functional groups on the SF flocs, by FTIR.

Still on Figure 4, can see as well the appearance and disappearance of peaks. A new peak appeared at 3012.28 cm^{-1} after the ionic flocculation process, which can be attributed to the presence of simple unsaturated olefinic compounds. This peak probably already existed before the ionic flocculation process but was hidden by the neighboring peak, which was minimized after the adsorption of MB causing the “new” peak to become visible. The peaks at 1711.78 , 623.91 and 488.68 cm^{-1} , which were there before the ionic flocculation, indicate the presence of simple carbonyl (possibly carboxyl) groups and the stretching of organic halides and polysulfides (S-S), respectively [35].

3.2. Effect of dosage and temperature

The surfactant dosage effect is a very important parameter to be studied, as it can influence the ability to change the effluent's pH, the equivalence of available adsorption sites and the release, or not, of secondary pollutants into the effluent. Figure 5 shows the SF dosage and temperature effects on the process.

Figure 5 shows that a greater SF dosage leads to a greater removal efficiency. This occurs due to the formation of more SF flocs and, consequently, the number of active sites available to adsorb MB molecules is also increased. Another possible reason for this behavior is the ability of MB to decrease the CMC of SF and contribute to the formation of micelles. The dissociation of the MB molecules present in the solution may be inserted into the polar part of the SF, promoting a reduction in the electrostatic repulsion of the SF micelles [36]. Similar results were found in the adsorption of MB by activated carbon [2], kaolin [10] and on the precipitation/flocculation of MB by calcium dodecyl sulfate [21].

Figure 5 also shows that temperature strongly influences the process. The removal efficiency increased as the process temperature decreased, which is a strong indication that the removal of MB by the SF flocs is an exothermic process. The removal efficiency decreased with increasing temperatures due to the increased SF solubility at higher temperatures, impairing the formation of SF flocs. Similar results were found for the removal of another dye (Reactive Blue 14) by ionic flocculation [37].

The best result obtained from the interaction between SF dosage and temperature was an MB removal of 84.14%, using an SF dosage of 4 g L^{-1} (considered the optimal dosage) at $10\text{ }^{\circ}\text{C}$. At room temperature ($30\text{ }^{\circ}\text{C}$)

and using the optimal dosage, the MB removal efficiency was 80%, proving that ionic flocculation is a highly efficient method even without adjusting the process temperature. This is still a great result as it avoids electricity expenditures, which also reduces the environmental impact of the process.

3.3. The pH effect

The pH directly affects the ionic flocculation process, as the surfactant has an anionic nature. Therefore, a strong sensitivity to pH variation is expected. Figure 6 shows the effect of pH on the ionic flocculation process.

From pH 12 upwards, MB presents a small change in its structure, as the MB peak shifts to 665 nm due to the high pH of the solution. In Figure 6, the removal of MB at $\text{pH} \geq 12$, without the addition of SF or calcium, illustrates this structural change in MB. Even though there is a 23% removal, MB is still in solution, not showing any increase in its removal efficiency. The addition of Ca^{2+} alone promotes an MB removal of 18.32%, which is lower than the lowest removal efficiency obtained by ionic flocculation (25.19%).

Figure 6 shows that ionic flocculation conducted at a $\text{pH} < 10$ has a maximal MB removal efficiency of 31.44%. This is due to SF's deprotonation at a pH close to neutral or acid. Due to the greater availability of H^+ ions, at these pH values SF undergoes a deprotonation and returns to its fatty acid state [37].

From a pH of 10 upwards (83.27% MB removal), there is a jump in the efficiency of the process until reaching the equilibrium state (pH 11, 93.71% MB removal). Above 11 (considered to be the optimal pH), the increase in pH had no influence on the MB removal efficiency. Similar results were observed for the removal of phenol [38] and malachite green dye [39] by ionic flocculation.

3.4. Effect of electrolytes

The analysis of the influence of electrolytes is an important step, as the presence of electrolytes can directly affect the ionic flocculation efficiency. Figure 7 shows the effect of electrolytes on the ionic flocculation process. NaCl concentrations greater than 0.5 mol L^{-1} cause the

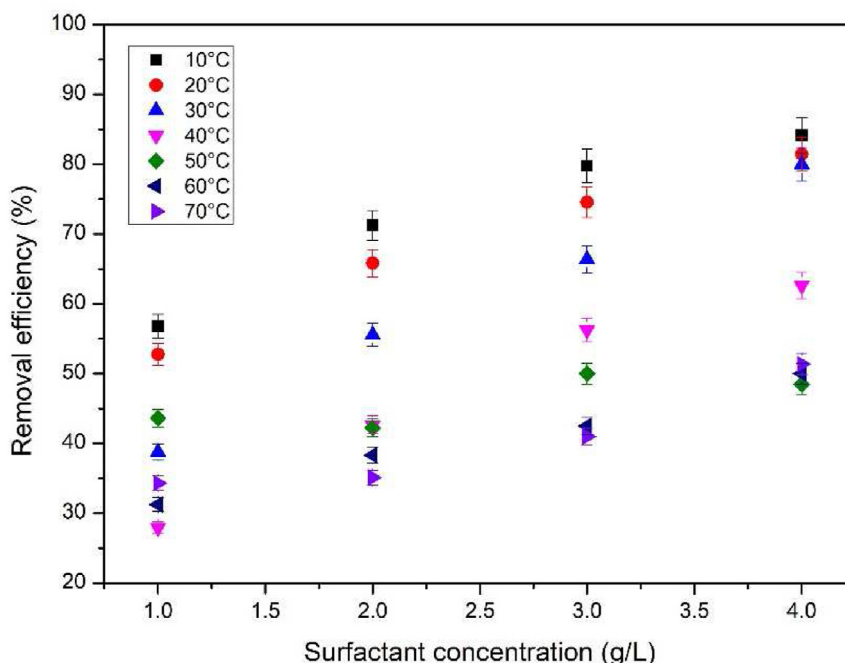


Figure 5. SF dosage and temperature effects (MB – 100 mg L^{-1} , NaCl – 0 mol L^{-1} , 90 min, pH 11, 20 mL, 80 rpm).

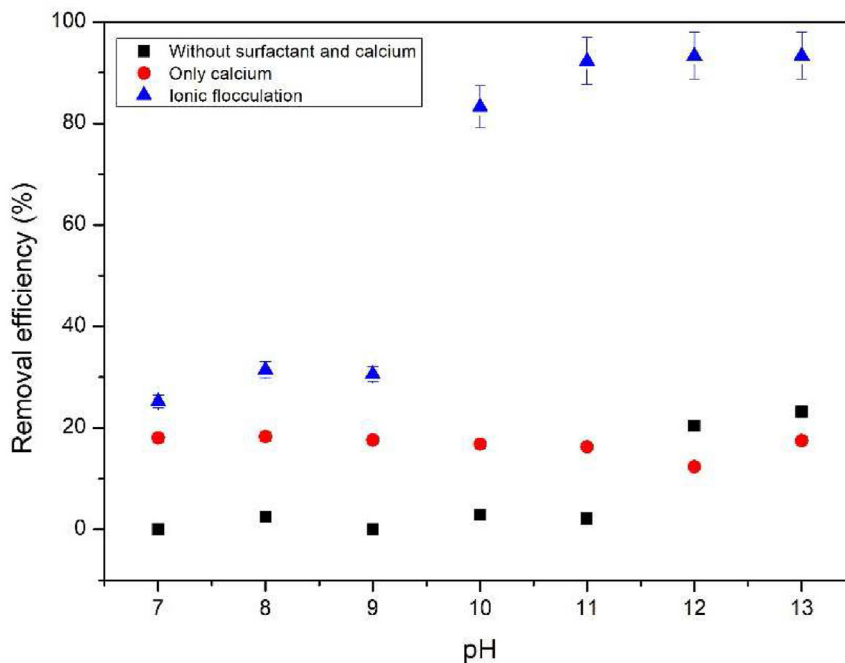


Figure 6. Effect of pH ($D_{SF} = 4 \text{ g L}^{-1}$, $MB = 100 \text{ mg L}^{-1}$, $NaCl = 0 \text{ mol L}^{-1}$, 90 min, 30 °C, 20 mL, 80 rpm).

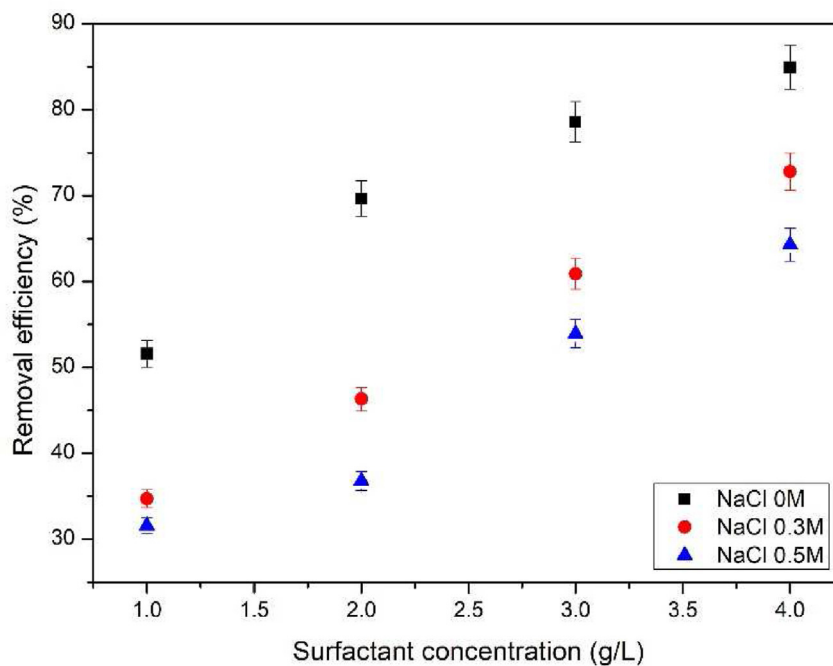


Figure 7. Effect of electrolytes ($MB = 100 \text{ mg L}^{-1}$, 90 min, pH 11, 30 °C, 20 mL, 80 rpm).

precipitation of SF even before the addition of Ca^{2+} , thus impairing the analysis of the process.

Figure 7 shows that the presence of electrolytes directly influences the ionic flocculation process regardless of SF dosage. As NaCl concentration increases, MB removal decreases. This is because the increased availability of Na^+ ions in the solution impairs the dissociation of SF, as the Na^+ ions themselves interact with SF [40, 41]. Consequently, the amount

of SF available to interact with Ca^{2+} decreases, also diminishing the formation of SF flocs, which ultimately are the ones responsible for the removal of MB.

The maximal removal of MB (84.93%) was reached at an SF dosage of 4 g L^{-1} and without any addition of NaCl. For the same dosage of SF with 0.3M NaCl, the removal rate dropped to 72.79%, while for 0.5M NaCl it dropped to 64.30%. The lowest MB removal rate (31.58%) was obtained

with an SF dosage of 1 g L^{-1} with 0.5 M NaCl . The same behavior was also observed with the removal of Reactive Blue 14 [37] and Direct Yellow 27 [42] by ionic flocculation.

3.5. Contact time

The study of the contact time makes it possible to verify the affinity of MB for the surface of the SF flocs. Figure 8 shows the influence the contact time has on the process.

As shown in Figure 8, the removal of MB decreases over time until an equilibrium level is reached, a behavior that was seen with all three MB concentrations assessed in this study. This occurs because the MB molecules, initially solubilized by the SF micelles, eventually migrate to the surface of the flocs formed by the addition of Ca^{2+} .

However, MB has its adsorption on the surface of the SF flocs affected by its hydrophilic nature, leading to a reduction in the efficiency of the process until it reaches equilibrium after 90 min. This type of behavior was also observed in the removal of Reactive Blue 14 by ionic flocculation [37].

The highest removal rates for the three MB concentrations assessed in this work were reached almost immediately (0.5 min). The removal rates for MB concentrations of 10, 50, 100 mg L^{-1} at that time were 96.94%, 96.66% and 93.71%, respectively. At equilibrium (90 min), the removal rates for MB concentrations of 10, 50, 100 mg L^{-1} were 91.94%, 89.91% and 79.98%, respectively.

The highest adsorption capacities for the three MB concentrations (10, 50, and 100 mg L^{-1}) were reached upon 0.5 min and were 2.42, 12.08 and 23.43 mg g^{-1} , respectively. At equilibrium (90 min), the adsorption capacities for MB concentrations of 10, 50, 100 mg L^{-1} were 2.30, 11.24 and 20 mg g^{-1} , respectively.

3.6. Adsorption isotherm

From the study of adsorption isotherms, it is possible to calculate the maximum adsorption capacity of the SF flocs, assess whether the adsorption process is favorable or not, and whether the process is a physisorption, ion exchange or chemisorption. Figure 9 shows the adsorption isotherm models evaluated for the process and Table 3 presents the parameters evaluated for each model.

Figure 9 and Table 3 show that the Langmuir and D-R adsorption isotherm models are the ones that best fit the results of this study (they are the two models with the highest R^2 and lowest RMSE). According to the Langmuir model, the process q_{max} is 101.38 mg g^{-1} and the adsorption of MB by the SF flocs is favored, as $0 < \text{RL} < 1$. According to the D-R model, the MB removal process by ionic flocculation occurs by chemical adsorption, or chemisorption, as $E > 16 \text{ kJ mol}^{-1}$. This last assumption is confirmed by the FTIR results, where it was possible to notice a decrease in intensity of some peaks and the disappearance of others, indicating that chemical bonds are formed between the SF flocs and MB.

The Langmuir model assumes that there is a certain given number of active sites with equivalent energies and that the molecules adsorbed on each site do not interact with each other. In addition, adsorption occurs as a monolayer formation process [43]. The D-R model assumes that the size of the adsorbent is comparable to the size of the micropore and that the adsorption equilibrium ratio does not depend on the temperature [44].

3.7. Adsorption thermodynamics

The spontaneity and nature of the process (exothermic or endothermic), as well as the decrease or increase in randomness in the system, can be determined through the thermodynamics tests. Table 4 shows the thermodynamic parameters obtained in the process.

Table 4 shows that, with the exception of an SF dosage of 1 g L^{-1} , all other tested dosages had equal or similar values of ΔH° and ΔS° . Negative values of ΔH° indicate that the MB adsorption process on the SF flocs is exothermic and, therefore, should expect for the removal of MB by ionic flocculation to be favored by a decrease in temperature. This result is in agreement with that shown in Figure 5.

The decrease in ΔS° with increasing SF dosages indicates that the disorder of the MB molecules retained on the SF flocs also decreases or, in other words, that the MB molecules are less randomly removed from the solution by the SF flocs. These results are in agreement with the thermodynamic theory involving adsorption processes, which states that the values of ΔH° and ΔS° must be both negative [44].

Negative ΔG° values indicate that the MB adsorption process by the SF flocs occurs spontaneously, whereas ΔG° positive values would

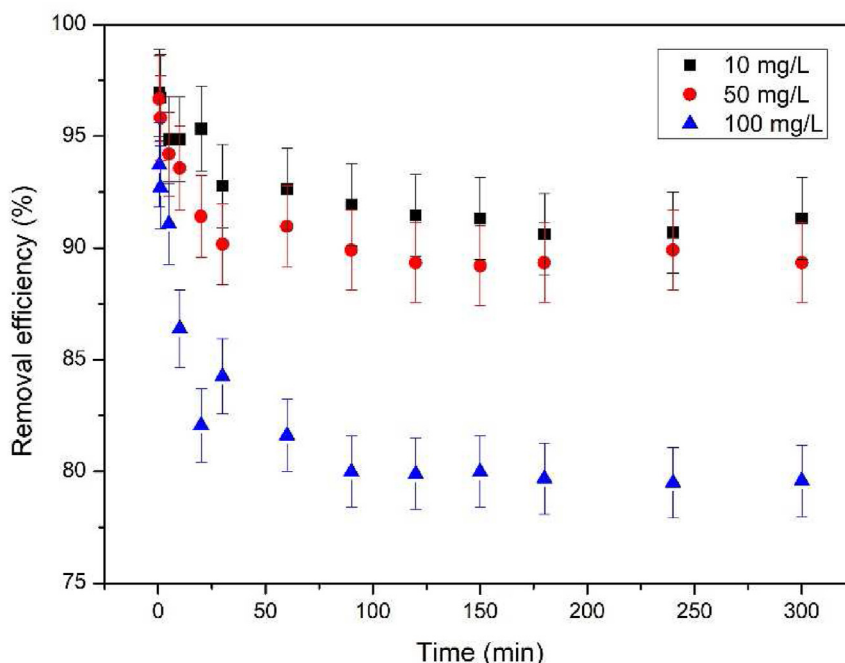


Figure 8. Contact time ($D_{\text{SF}} = 4 \text{ g L}^{-1}$, $\text{NaCl} = 0 \text{ mol L}^{-1}$, $\text{pH} = 11$, 30°C , 20 mL , 80 rpm).

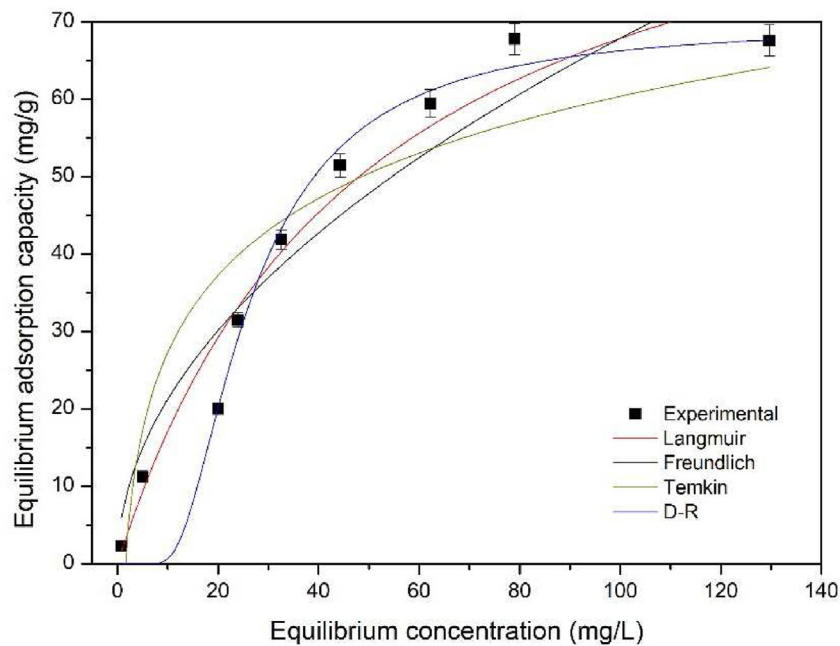


Figure 9. Adsorption isotherm models ($D_{SF} = 4 \text{ g L}^{-1}$, $\text{NaCl} = 0 \text{ mol L}^{-1}$, 90 min, pH 11, 30 °C, 20 mL, 80 rpm).

Table 3. Adsorption isotherm parameters.

Dye	T (°C)	Langmuir					D-R				
		q_{max} (mg g ⁻¹)	k_L (L mg ⁻¹)	RL^a	R^2	RMSE	q_m (mg g ⁻¹)	k_{DR} (mol ² kJ ⁻²)	E (kJ mol ⁻¹)	R^2	RMSE
MB	30	101.38	0.02	0.33	0.96	4.45	69.78	8.23E-5	77.94	0.96	4.21
		Freundlich									
		b (J mol ⁻¹)	k_F (L mg ⁻¹)	R^2	RMSE	k_F (L mg ⁻¹)	n	R^2	RMSE		
		0.67	175.34	0.83	8.87	6.63	1.98	0.91	6.45		

^a Initial MB concentration: 100 mg L⁻¹.

indicate a non-spontaneous process. The results presented in Table 4 show that the spontaneity of the process directly depends on temperature and SF dosage.

Increasing SF dosages leads to an increase in the spontaneity of the process, while a decrease in the SF dosage causes the MB adsorption on the SF flocs to occur non-spontaneously, requiring, because of its exothermic nature, a reduction in temperature for the process to occur.

3.8. Desorption kinetics and efficiency

The study of desorption is important to evaluate the recyclability and reuse of SF flocs as an adsorbent for more than one cycle. Figure 10 shows the kinetics and efficiency of the MB desorption from the SF flocs after the adsorption process has already occurred. The eluents HCl (0.1 mol L⁻¹) and HCl (0.01 mol L⁻¹) cause the destruction of the SF flocs (data not shown), making the use of these eluents unfeasible. The flocs used in

Table 4. Thermodynamic parameters.

D_{SF} (g L ⁻¹)	Temp. (°C)	ΔG° (kJ mol ⁻¹)	ΔH° (kJ mol ⁻¹)	ΔS° (kJ mol ⁻¹ K ⁻¹)	D_{SF} (g L ⁻¹)	Temp. (°C)	ΔG° (kJ mol ⁻¹)	ΔH° (kJ mol ⁻¹)	ΔS° (kJ mol ⁻¹ K ⁻¹)
1	10	-0.28	-12.98	-0.04	3	10	-3.22	-25.08	-0.08
1	20	0.17			3	20	-2.45		
1	30	0.62			3	30	-1.68		
1	40	1.07			3	40	-0.90		
1	50	1.51			3	50	-0.13		
1	60	1.96			3	60	0.64		
1	70	2.41			3	70	1.41		
2	10	-2.01	-21.49	-0.07	4	10	-4.17	-26.87	-0.08
2	20	-1.32			4	20	-3.37		
2	30	-0.63			4	30	-2.57		
2	40	0.06			4	40	-1.77		
2	50	0.74			4	50	-0.96		
2	60	1.43			4	60	-0.16		
2	70	2.12			4	70	0.64		

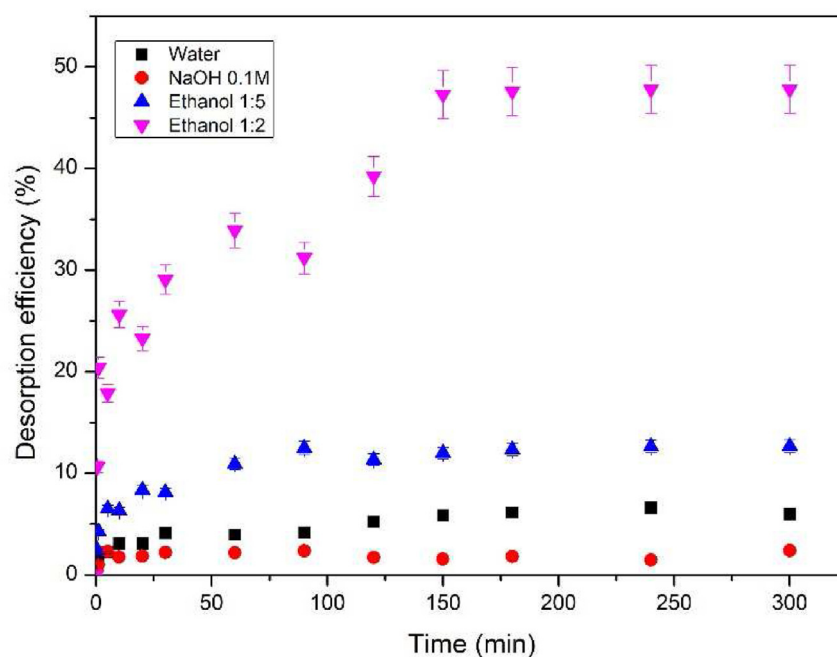


Figure 10. Desorption kinetics and efficiency ($SF = 4 \text{ g L}^{-1}$, $NaCl = 0 \text{ mol L}^{-1}$, $30 \text{ }^\circ\text{C}$, 20 mL , 80 rpm).

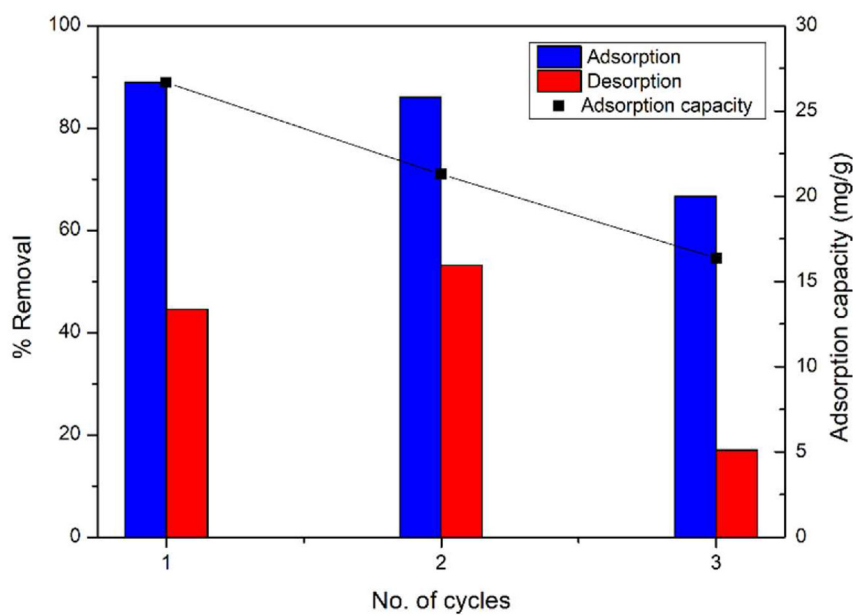


Figure 11. Adsorption-Desorption cycles of MB (Eluent - ethanol 1:2).

Table 5. Comparison of ionic flocculation with previous studies.

Method	MB (mg L^{-1})	MB removal efficiency (%)	MB removal cap. (mg L^{-1})	Max. ads. cap. (mg g^{-1})	Reference
Ionic Flocculation	100	93.71	93.71	101.38	This work
Flocculation	50	98.63	49.32	Unstudied	20
Flocculation	90	98.99	89.09	Unstudied	46
Adsorption	20	90.00	18.00	35.70	22
Adsorption	100	97.50	97.50	52.76	10
Ultrafiltration	6	99.30	5.96	Unstudied	18
Ultrafiltration	5	94.33	4.72	Unstudied	19

the kinetic desorption study and adsorption-desorption cycles (Figure 11) contained 26.67 mg-MB g⁻¹.

Figure 10 shows that the least efficient eluent is NaOH (0.1M) and the most efficient one is the ethanol 1:2 solution. The maximal desorption efficiencies using NaOH (0.1M), deionized water (pH = 5.54), ethanol 1:5, and ethanol 1:2 were 2.41%, 6.59%, 12.68% and 47.81%, respectively.

The desorption kinetics reached a state of equilibrium for all eluents starting at 150 min from contact, which is an excellent result as it shows that there is no need to wait long periods of time to promote the regeneration of the SF flocs.

Ethanol 1:2 was able to desorb much of the MB present on the flocs' surface, leaving only the MB adsorbed within the flocs' macro and micropores. The hydrophobic interaction between the MB molecules and the ethanol molecules leads to an increase in the solubility of MB, reducing the amount of MB adsorbed on the SF flocs and increasing the desorption efficiency. Similar results were obtained for the desorption of MB on agar [45].

Figure 11 shows the adsorption-desorption efficiencies and the adsorption capacity of the SF flocs for three cycles. After three consecutive cycles, the adsorption efficiency decreased from 88.91% to 66.67% while the desorption efficiency decreased from 44.59% to 17%. This reduction occurs due to the increase of irreversible interactions between MB and the SF flocs. Consequently, the adsorption capacity of the flocs also decreases with increasing cycles, being 26.67 mg g⁻¹ in the first cycle and 16.37 mg g⁻¹ in the third cycle. Recyclability studies suggest that the SF flocs generated in the ionic flocculation and already impregnated by the dye can still be regenerated and effectively used to remove MB from the solution.

3.9. Comparison with other studies

Table 5 was constructed in order to compare the ionic flocculation removal efficiency and the adsorption capacity of the SF flocs with other studies found in the literature using MB as a model pollutant.

From Table 5, it can be concluded that ionic flocculation using frying soybean oil as surfactant provides a high MB removal efficiency and that the SF flocs have a high MB adsorption capacity, which indicates a potential similar to that shown by previous studies.

In addition, the treated effluent was analyzed in order to identify contamination by secondary pollutants (residual Ca²⁺). The hardness analysis through complexation volumetry using EDTA showed a result of approximately 34.50 ± 4.27 mg-CaCO₃ L⁻¹. Therefore, the treated effluent has a low hardness (soft water) and, consequently, a small amount of secondary pollutants, indicating that ionic flocculation using a surfactant originated from frying soybean oil is an ecologically sound process and a strong contributor to sustainable technologies.

4. Final considerations

In this work, frying soybean oil was used as raw material to promote ionic flocculation as a treatment of a synthetic effluent contaminated with MB. SF flocs have OH⁻ and C=O functional groups, which promote the adsorption of the dissolved MB. SF dosage and temperature directly influence MB removal, while the removal efficiency increases when the SF concentration is increased and the process temperature decreases. High pH values (pH > 9) lead to the best MB removal results, while the presence of electrolytes decreases the efficiency of the process. Equilibrium is reached in 90 min. The isotherm models that best fitted the results of this study are the Langmuir (q_{max} = 101.38 mg g⁻¹) and D-R models, indicating that we are in the presence of a chemisorption process. The adsorption of MB on SF flocs has an exothermic nature (-ΔH°). The best eluent to promote MB desorption from the SF flocs is an ethanol 1:2 solution. With an MB removal efficiency of up to 93.71% for an initial MB concentration of 100 mg L⁻¹, ionic flocculation promoted by a surfactant obtained from

frying soybean oil is a promising process for the treatment of effluents containing cationic dyes such as MB.

Declarations

Author contribution statement

Yago Neco Teixeira: Conceived and designed the experiments; Performed the experiments; Wrote the paper.

Vinicius Pereira Bacurau: Performed the experiments; Conceived and designed the experiments; Wrote the paper.

Anderson Zhong Fan: Performed the experiments; Analyzed and interpreted the data.

Jorge Marcell Coelho Menezes: Performed the experiments; Analyzed and interpreted the data; Wrote the paper.

Ricardo Paulo Fonseca Melo: Analyzed and interpreted the data; Wrote the paper.

Francisco José de Paula Filho: Analyzed and interpreted the data; Contributed reagents, materials, analysis tools or data; Wrote the paper.

Funding statement

This work was supported by Fundação Cearense de Apoio ao Desenvolvimento Científico e Tecnológico (Grant No BP3-0139-00276.01.00/18) and (Grant No BP4-0172-00080.01.00/20) and Coordenação de Aperfeiçoamento de Pessoal de Nível Superior (Grant No 88887.613868/2021-00).

Data availability statement

Data included in article/supp. material/referenced in article.

Declaration of interest's statement

The authors declare no conflict of interest.

Additional information

No additional information is available for this paper.

References

- [1] M. Tichonovas, E. Krugly, V. Racys, R. Hippler, V. Kauneliene, I. Stasiulaitiene, D. Martuzevicius, Degradation of various textiles dyes as wastewater pollutants under dielectric barrier discharge plasma treatment, *Chem. Eng. J.* 229 (2013) 9–19.
- [2] M. Mariana, E.M. Mistar, T. Alfatah, M.D. Supardan, High-porous activated carbon derived from *Myristica fragrans* shell using one-step KOH activation for methylene blue adsorption, *Bioresour. Technol. Rep.* 16 (2021) 100845.
- [3] A.R. Disanto, J.G. Wagner, Pharmacokinetics of highly ionized drugs I: methylene blue—whole blood, urine, and tissue assays, *J. Pharm. Sci.* 61 (1972) 598–602.
- [4] M. Oz, D.E. Lorke, M. Hasan, G.A. Petroianu, Cellular and molecular actions of Methylene Blue in the nervous system, *Med. Res. Rev.* 31 (1) (2010) 93–117.
- [5] G.V. Brião, S.L. Jahn, E.L. Foletto, G.L. Dotto, Highly efficient and reusable mesoporous zeolite synthesized from a biopolymer for cationic dyes adsorption, *Colloid Surf. A-Physicochem. Eng. Asp.* 556 (2018) 43–50.
- [6] P. Yilmaz, D. Gunduz, B. Ozbek, Utilization of low-cost bio-waste adsorbent for methylene blue dye removal from aqueous solutions and optimization of process variables by response surface methodology approach, *Desalination Water Treat.* 224 (2021) 367–388.
- [7] M.I. Khan, T.K. Min, K. Azizli, S. Sufian, H. Ullah, Z. Man, Effective removal of methylene blue from water using phosphoric acid based geopolymers: synthesis, characterizations and adsorption studies, *RSC Adv.* 5 (2015) 61410–61420.
- [8] M. Rafatullah, O. Sulaiman, R. Hashim, A. Ahmad, Adsorption of methylene blue on low-cost adsorbents: a review, *J. Hazard Mater.* 177 (1–3) (2010) 70–80.
- [9] R.M. Novais, G. Ascensão, D.M. Tobaldi, M.P. Seabra, J.A. Labrincha, Biomass fly ash geopolymer monoliths for effective methylene blue removal from wastewaters, *J. Clean. Prod.* 171 (2018) 783–794.
- [10] L. Mouni, L. Belkhir, J.C. Bollinger, A. Bouzaza, A. Assadi, A. Tirri, F. Dahmoune, K. Madani, H. Remini, Removal of Methylene Blue from aqueous solutions by adsorption on Kaolin: kinetic and equilibrium studies, *Appl. Clay Sci.* 153 (2018) 38–45.

- [11] G. Son, D. Kim, J.S. Lee, H. Kim, C. Lee, S.R. Kim, H. Lee, Synchronized methylene blue removal using Fenton-like reaction induced by phosphorous oxoanion and submerged plasma irradiation process, *J. Environ. Manag.* 206 (2018) 77–84.
- [12] Y. Pan, X. Shi, P. Cai, T. Guo, Z. Tong, H. Xiao, Dye removal from single and binary systems using gel-like bioadsorbent based on functional-modified cellulose, *Cellulose* 25 (2018) 2559–2575.
- [13] X.S. Hu, R. Liang, G. Sun, Superadsorbent hydrogel for removal of methylene blue dye from aqueous solution, *J. Mater. Chem. A* 6 (2018) 17612–17624.
- [14] N. Somsessa, V. Sricharoenchaikul, D. Aht-Ong, Adsorption removal of methylene blue onto activated carbon/cellulose biocomposites films: equilibrium and kinetic studies, *Mater. Chem. Phys.* 240 (2020) 122221.
- [15] M.P. González, M.M. Luna, J.S. Salazar, H.C. Ledesma, P.E.G. Tinoco, S.A. Tomás, Improved adsorption and photocatalytic removal of methylene blue by MoO₃ thin films: role of the sputtering power, film thickness, and sputtering working pressure, *Catal. Today* 360 (2021) 138–146.
- [16] J. Cheng, C. Zhan, J. Wu, Z. Cui, J. Si, Q. Wang, X. Peng, L.S. Turng, Highly efficient removal of methylene blue dye from an aqueous solution using cellulose acetate nanofibrous membranes modified by polydopamine, *ACS Omega* 5 (2020) 5389–5400.
- [17] N. Benosmane, B. Boutemeur, S.M. Hamdi, M. Hamdi, Removal of methylene blue dye from aqueous solutions using polymer inclusion membrane technology, *Appl. Water Sci.* 12 (2022) 104.
- [18] J.H. Huang, C.F. Zhou, G.M. Zeng, X. Li, J. Niu, H.J. Huang, L.J. Shi, S.B. He, Micellar-enhanced ultrafiltration of methylene blue from dye wastewater via a polysulfone hollow fiber membrane, *J. Membr. Sci.* 365 (2010) 138–144.
- [19] M. Bielska, J. Szymanowski, Removal of methylene blue from waste water using micellar enhanced ultrafiltration, *Water Res.* 40 (2006) 1027–1033.
- [20] P.J. Quinlan, A. Tanvir, K.C. Tam, Application of the central composite design to study the flocculation of an anionic azo dye using quaternized cellulose nanofibrils, *Carbohydr. Polym.* 133 (2015) 80–89.
- [21] Z. Yang, M. Li, M. Yu, J. Huang, H. Xu, Y. Zhou, P. Song, R. Xu, A novel approach for methylene blue removal by calcium dodecyl sulfate enhanced precipitation and microbial flocculant GA1 flocculation, *Chem. Eng. J.* 303 (2016) 1–13.
- [22] A.G. Rêgo Júnior, G.A.S. Nobrega, R.C.L. Silva, D.A.A. Gomes, Study of the removal of methylene blue dye from aqueous solutions using in natura bamboo (*Bambusa Vulgaris*) as adsorbent, *Res., Soc. Dev.* 11 (6) (2022), e46711629314.
- [23] P. Su, Q. Wan, Y. Yang, J. Shu, H. Zhao, W. Meng, B. Li, M. Chen, Z. Liu, R. Liu, Hydroxylation of electrolytic manganese anode slime with EDTA-2Na and its adsorption of methylene blue, *Separ. Purif. Technol.* 278 (2021), 119526.
- [24] J. Shu, R. Liu, H. Wu, Z. Liu, X. Sun, C. Tao, Adsorption of methylene blue on modified electrolytic manganese residue: kinetics, isotherm, thermodynamics and mechanism analysis, *J. Taiwan Inst. Chem. Eng.* 82 (2018) 351–359.
- [25] R.P.F. Melo, E.L. Barros Neto, M.C.P.A. Moura, T.N. Castro Dantas, A.A. Dantas Neto, S.K.S. Nunes, Removal of direct Yellow 27 dye by ionic flocculation: the use of an environmentally friendly surfactant, *J. Surfactants Deterg.* 20 (2017) 459–465.
- [26] D. Myers, *Surfactant Science and Technology*, John Wiley & Sons, USA, 2006.
- [27] D. Daltin, *Tensoativos: Química, propriedades e aplicações*, Blucher, Brazil, 2011.
- [28] A. Zapf, R. Beck, G. Platz, H. Hoffmann, Calcium surfactants: a review, *Adv. Colloid Interface Sci.* 100–102 (2003) 349–380.
- [29] C.H. Niebish, A.K. Malinowski, R. Schadeck, D.A. Mitchell, V. Kava-Cordeiro, J. Paba, Decolorization and biodegradation of reactive blue 220 textile dye by *Lentinus crinitus* extracellular extract, *J. Hazard Mater.* 180 (2010) 316–322.
- [30] R.F. Nascimento, A.C.A. Lima, C.B. Vidal, D.Q. Melo, G.S.C. Raulino, *Adsorção: Aspectos teóricos e aplicações ambientais*, Imprensa Universitária, Brazil, 2020.
- [31] A. Kaveeshwar, E. Revellame, D.D. Gang, R. Subramaniam, Adsorption properties and mechanism of barium (II) and strontium (II) removal from fracking wastewater using pecan shell based activated carbon, *J. Clean. Prod.* 193 (2018) 1–13.
- [32] A. Nasrullah, A.H. Bhat, A. Naem, M.H. Isa, M. Danish, High surface area mesoporous activated carbon-alginate beads for efficient removal of methylene blue, *Int. J. Biol. Macromol.* 107 (2018) 1792–1799.
- [33] A. Benhouria, M.A. Islam, H. Zaghouane-Boudiaf, M. Boutahala, B. Hameed, Calcium alginate–bentonite–activated carbon composite beads as highly efficient adsorbent for methylene blue, *Chem. Eng. J.* 270 (2015) 621–630.
- [34] M.E.S. Mirghani, Y.B. Che Man, S. Jinap, B.S. Baharin, J. Bakar, FTIR spectroscopic determination of soap in refined vegetable oils, *J. Am. Oil Chem. Soc.* 79 (2002) 111–116.
- [35] A.B.D. Nadiyanto, R. Oktiani, R. Ragadhita, How to read and interpret FTIR spectroscopy of organic material, *Indones. J. Sci. Technol.* 4 (2019) 97–118.
- [36] J.H. Huang, C.F. Zhou, G.M. Zeng, X. Li, J. Niu, H.J. Huang, L.J. Shi, S.B. He, Micellar-enhanced ultrafiltration of methylene blue from dye wastewater via a polysulfone hollow fiber membrane, *J. Membr. Sci.* 365 (2010) 138–144.
- [37] R.P.F. Melo, E.L. Barros Neto, S.K.S. Nunes, T.N. Castro Dantas, A.A. Dantas Neto, Removal of Reactive Blue 14 dye using micellar solubilization followed by ionic flocculation of surfactants, *Separ. Purif. Technol.* 191 (2018) 161–166.
- [38] P.R.M. Cavalcante, R.P.F. Melo, T.N. Castro Dantas, A.A. Dantas Neto, E.L. Barros Neto, M.C.P.A. Moura, Removal of phenol from aqueous medium using micellar solubilization followed by ionic flocculation, *J. Environ. Chem. Eng.* 6 (2018) 2778–2784.
- [39] Y.N. Teixeira, P.R.F. Melo, M.R. Fernandes, S.K.S. Carmo, E.L. Barros Neto, Malachite green removal using ionic flocculation, *Water Pract. Technol.* 17 (2022) 1113.
- [40] K.L. Stellner, J.F. Scamehorn, Hardness tolerance of anionic surfactant solutions. 1. Anionic surfactant with added monovalent electrolyte, *Langmuir* 5 (1989) 70–77.
- [41] C. Noik, M. Bavière, D. Defives, Anionic surfactant precipitation in hard water, *J. Colloid Interface Sci.* 115 (1987) 36–45.
- [42] R.P.F. Melo, E.L. Barros Neto, M.C.P.A. Moura, T.N. Castro Dantas, A.A. Dantas Neto, H.N.M. Oliveira, Removal of direct Yellow 27 dye using animal fat and vegetable oil-based surfactant, *J. Water Proc. Eng.* 7 (2015) 196–202.
- [43] A. Bonilla-Petriciolet, D.I. Mendonza-Castillo, H.E. Reynel-Ávila, *Adsorption Processes for Water Treatment and Purification*, Springer, Switzerland, 2017.
- [44] D.M. Ruthven, *Principles of Adsorption and Adsorption Processes*, John Wiley & Sons, USA, 1984.
- [45] B. Samiey, F. Ashoori, Adsorptive removal of methylene blue by agar: effects of NaCl and ethanol, *Chem. Cent. J.* 6 (2012) 1–13.
- [46] S. Ihaddaden, D. Aberkane, A. Boukerrouj, D. Robert, Removal of methylene blue (basic dye) by coagulation-flocculation with biomaterials (bentonite and *Opuntia ficus indica*), *J. Water Proc. Eng.* 49 (2022) 102952.